remote sensing

MDPI

Technical Note

A New Method of Electron Density Retrieval from MetOp-A's Truncated Radio Occultation Measurements

M. Mainul Hoque [1,*], Liangliang Yuan [1], Fabricio S. Prol [1,2], Manuel Hernández-Pajares [3], Riccardo Notarpietro [4], Norbert Jakowski [1], German Olivares Pulido [3], Axel Von Engeln [4] and Christian Marquardt [4]

[1] German Aerospace Center (DLR), Institute for Solar-Terrestrial Physics, Kalkhorstweg 53, 17235 Neustrelitz, Germany
[2] Department of Navigation and Positioning, Finnish Geospatial Research Institute (FGI), National Land Survey of Finland (NLS), Vuorimiehentie 5, 02150 Espoo, Finland
[3] Department of Mathematics, Universitat Politècnica de Catalunya—IOnospheric Determination and Navigation Based on Satellite and Terrestrial Systems (UPC-IonSAT), E08034 Barcelona, Spain
[4] European Organisation for the Exploitation of Meteorological Satellites (EUMETSAT), Eumetsat Allee 1, 64295 Darmstadt, Germany
* Correspondence: mainul.hoque@dlr.de; Tel.: +49-3981-480-125

Abstract: The radio occultation (RO) measurements of the Global Navigation Satellite System's (GNSS's) signals onboard a Low Earth Orbiting (LEO) satellite enable the computation of the vertical electron density profile from the LEO satellite's orbit height down to the Earth's surface. The ionospheric extension experiment performed by the GNSS Receiver for Atmospheric Sounding (GRAS) receiver on board MetOp-A provides opportunities for ionospheric sounding but with the RO measurements only taken with an impact parameter height below 600 and 300 km within two different experiments, although MetOp-A was flying at an orbit height of about 800 km. Here, we present a model-assisted RO inversion technique for electron density retrieval from such kind of truncated data. The topside ionosphere and plasmasphere above the LEO orbit height are modelled by a Chapman layer function superposed with an exponential decay function representing the plasmasphere. Our investigation shows that the model-assisted technique is stable and robust and can successfully be used to retrieve the electron density values up to the LEO height from the truncated MetOp-A data, in particular when observations are available until 600 km. Moreover, this model-assisted technique is also successful with the availability of a small number of observations of the topside above the peak density height. For observations available only up to 300 km, the accuracy of the retrieved profile is comparable to the one obtained by the data truncated at a 600 km height only when the peak electron density lies below the 250 km altitude level.

Keywords: GNSS radio occultation; Abel inversion; MetOp-A extension campaign; electron density retrieval from truncated data

Citation: Hoque, M.M.; Yuan, L.; Prol, F.S.; Hernández-Pajares, M.; Notarpietro, R.; Jakowski, N.; Olivares Pulido, G.; Von Engeln, A.; Marquardt, C. A New Method of Electron Density Retrieval from MetOp-A's Truncated Radio Occultation Measurements. *Remote Sens.* **2023**, *15*, 1424. https://doi.org/10.3390/rs15051424

Academic Editor: Michael E. Gorbunov

Received: 30 January 2023
Revised: 25 February 2023
Accepted: 27 February 2023
Published: 3 March 2023

1. Introduction

The radio occultation (RO) measurements of the Global Navigation Satellite System's (GNSS's) signals, recorded onboard a LEO satellite, allow for the vertical sounding of the terrestrial atmosphere and ionosphere. Accurate and very well vertically resolved temperature and humidity profiles in the neutral atmosphere can be retrieved by processing such measurements. In a similar way, RO soundings are also capable of providing information on the vertical structure of the electron density if the measurements cover an appropriate height range (e.g., 90–600 km) [1–3]. In the framework of the MetOp-A end-of-life testing campaign, the EUMETSAT (the European Organisation for the Exploitation of Meteorological Satellites) conducted an ionospheric extension experiment enabling the GNSS Receiver for Atmospheric Sounding (GRAS) instrument to extend its vertical measurement range

for ionosphere soundings for a three-month period during the summer of 2020. During the test campaign, a large set of Global Positioning System (GPS) radio occultation measurements (e.g., carrier phases and pseudo ranges) was recorded by the GRAS instrument. The ionospheric measurements were taken during two different experiments, with an impact parameter height below 600 km and 300 km, whereas the MetOp-A was flying at an orbit height of about 800 km.

Radio occultation measurements enable the computation of the vertical electron density profile from the LEO satellite's height down to the Earth's surface. In general, the derived profile is a horizontally averaged one. However, by considering the effect of the non-spherical electron density distributions along the propagation path, a more accurate electron density profile can be retrieved [1,2]. Apart from the effect of the non-spherical electron density distributions, the GNSS-to-LEO occultation poses another problem: the transmitter is outside the plasmapause, but the receiver is in the ionosphere. We have to eliminate the slant electron content of the plasmasphere and the upper ionosphere above the LEO orbit height [3,4] for an accurate electron density retrieval. Since MetOp-A's RO measurements are not available up to the satellite's orbit, there are two main concerns that make the electron density reconstruction very challenging: (1) the plasmaspheric contribution above 600/300 km up to the GNSS's orbit height needs to be correctly modelled and estimated and removed, and (2) the topside electron density above 600/300 km up to the MetOp-A's orbit height needs to be extrapolated. Some aspects of the electron density retrieval and its impact on the EUMETSAT's Polar System-Second Generation, or EPS-SG, were already studied by Hernández-Pajares et al. [5] and Lyu et al. [6]. Hernández-Pajares et al. [5] developed a technique based on the vary-Chapman extrapolation, provided that the electron density profile is properly estimated up to the truncation height. As a consequence of this research, the overall technique, the Abel-VaryChap Hybrid density profile, from topside Incomplete RO data (AVHIRO), was developed and later compared with the estimation of the electron density profile from the topside Incomplete RO data (SEEIRO) technique [5,6]. Lyu et al. [6] found that the AVHIRO technique outperformed the SEEIRO technique in terms of accuracy, although the computational time per occultation was found to be too high (e.g., 20 min) for any near real-time application.

Being aware that AVHIRO requires high computational power, an improved version has been developed. One potential way of reducing the search time to solve AVHIRO's non-linear equations may be to consider, as an initial guess, the climatological model of the linear VaryChap parameters developed in [5] after analyzing several years of topside sounders and the GNSS RO data. This is exactly performed in AVHIRO2. AVHIRO2 is a new way of combining the Abel inversion and the Chapman model with a linearly increasing scale height to retrieve ionospheric electron density vertical profiles from truncated RO data gathered by the onboard LEO GNSS receivers. The results, tested on a set of representative GNSS RO measured by COSMIC/FORMOSAT-3, show that this method can retrieve an electron density profile with a predominant absolute and relative error of 10^{10} m^{-3} and 5%, respectively, within a few seconds of the computational time, which makes this method suitable for near real-time applications in upcoming missions, such as the EPS-SG.

We have presented here a model-assisted RO inversion technique for electron density retrieval from truncated RO data. The topside ionosphere and plasmasphere above the LEO orbit height were modelled by a Chapman layer function superposed with an exponential decay function, as described in the following Section 2. The technique is validated against reference RO profiles from the COSMIC-1 mission [7,8] in Section 3. Section 3 also includes the first results of the RO retrievals from MetOp-A's truncated data. Finally, the new findings are concluded in Section 4.

2. Adaptive Topside Ionosphere–Plasmasphere Model's Technique

Jakowski et al. [3] were the first to consider an extrapolation approach for retrieving RO profiles from CHAMP and GRACE satellite data, which flew at relatively lower orbit heights (e.g., 400–450 km). We adopted a similar technique for retrieving electron density

profiles from MetOp-A's truncated data. It is a model-assisted technique where the topside ionosphere and plasmasphere above the LEO orbit height are modelled by a Chapman layer function superposed with an exponential decay function representing the plasmasphere. The ionospheric electron density distribution, *Ne*, along the height, *h*, can be written by a Chapman layer [9] and an exponential decay function [4] as

$$Ne(h) = N_{eF} + N_{eP} \tag{1}$$

$$N_{eF} = Nm{\cdot}exp(0.5(1 - z - exp(-z))) \tag{2}$$

$$N_{eP} = np{\cdot}exp(-z_p) \tag{3}$$

$$z = \frac{h - hm}{Hs}$$

$$z_p = \frac{h - hm}{Hsp}$$

where *Hs* is the atmospheric scale height, *Nm* is the peak ionization, and *hm* is the corresponding height of the peak ionization of the Chapman layer. The quantity, *Hsp*, is the plasmaspheric scale height. The quantity, *np*, is the plasmaspheric basic density and is assumed to be proportional to the peak density, *Nm* [4]. The plasmaspheric density is maximum at the F2 layer peak ionization height, *hm*, and exponentially decreases with the increase in height. It should be noted that the plasmaspheric density below the F2 peak is assumed to be zero.

An example of a Chapman layer with and without the inclusion of an exponential decay function is given in the left panel of Figure 1. The corresponding scale heights are computed by the following equation (see [10]), with the known *Hs*0 = 70 km, and plotted in the right panel of Figure 1.

$$Hs = \frac{h - hm}{1 - 2ln\left(\frac{N_e}{Nm}\right) - exp\left(\frac{-h-hm}{Hs0}\right)} \tag{4}$$

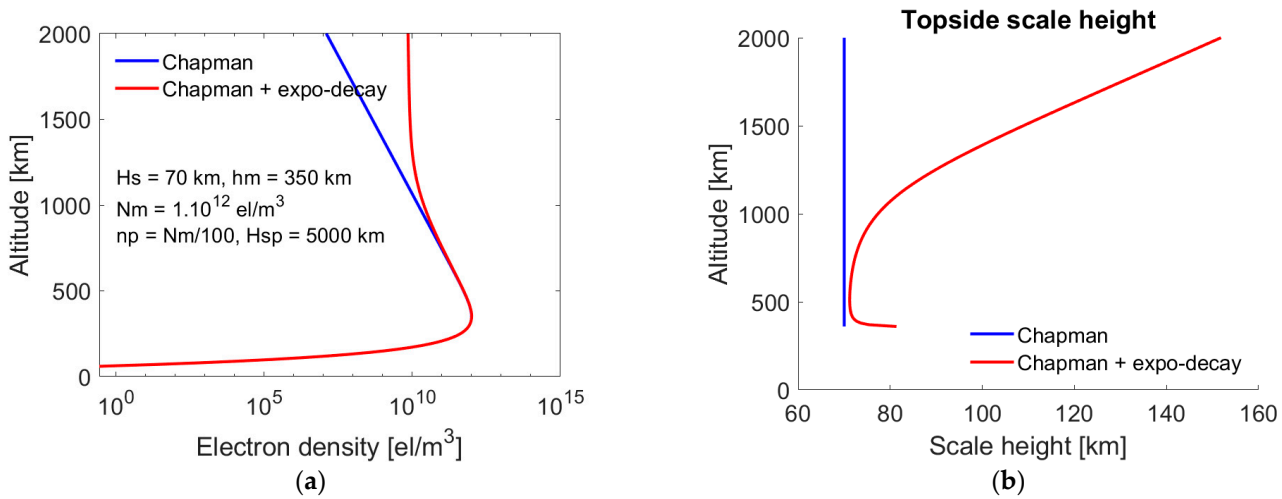

Figure 1. Left (Plot (**a**)): Sample electron density profiles using a Chapman layer and one in combination with an exponential decay function. Right (Plot (**b**)): variation of scale height as a function of altitude derived from the Chapman and combined profiles.

The literature studies (e.g., Refs. [1–6,11]) show that the topside ionosphere–plasmasphere scale height increases nearly linearly with the altitude. Considering this, a vary-Chapman function is often used for topside ionosphere–plasmasphere modelling. The vary-Chapman function uses a Chapman layer with a variable scale height. However, here we have modelled

the topside ionosphere–plasmasphere by a Chapman layer superposed by an exponential decay function. As Figure 1 shows, the topside scale height above the 1000 km altitude increases nearly linearly for the combined model composed of a Chapman layer and an exponential decay function. It is noted that, for simplicity, the topside ionosphere is approximated by electron density profile functions with a linear dependence on the scale height. However, the validity of such an assumption was not well-investigated above the 800 km altitude due to the lack of observational data. Recently, Prol et al. [11] investigated the ionospheric scale height using Van Allen Probes data and found the dependence of the scale heights on the altitude as quadratic rather than linear in the upper altitude (>1000 km). The assumption of a linear scale height is indeed in contrast with the recent results. The use of a nonlinear scale height model will improve the RO inversion results; however, such a model is not yet available.

The above-mentioned ionosphere and plasmasphere model parameters (e.g., *Nm*, *hm*, *Hs*, and *np*) are derived by an iterative approach by fitting the model functions to the RO data. Practically, the solution starts with the first measurement at the maximum tangential height. The RO reconstruction steps can be summarized as follows:

1. The slant total electron content (sTEC) profile of an occultation event is derived from the dual-frequency carrier phase measurements by

$$sTEC = \frac{f_1^2 f_2^2}{40.3\left(f_1^2 - f_2^2\right)}(\Phi_1 - \Phi_2) + B_{ambiguity} - bias^{satellite,receiver} \quad (5)$$

   where Φ_1 and Φ_2 denote the carrier phase observations at f_1 and f_2 frequencies, respectively, and $B_{ambiguity}$ is the carrier phase ambiguity term. The computed sTEC is biased by a constant ambiguity and an inter-frequency phase bias term.

2. The sTEC contribution of the plasmasphere and the upper ionosphere above the LEO orbit height is first removed. Partially, this is conducted by subtracting from all the data the sTEC measured for the upper end of the occultation (for the highest occultation ray perigee). The common ambiguity and bias terms are also removed in such an approach. It should be noted that the topside ionospheric and plasmaspheric electron content (PEC) contributions for the outer LEO-to-GNSS paths are not the same for all the rays (e.g., the PEC is not the same for the AA' and HH' ray paths in Figure 2). The differences in the PEC need to be mitigated for accurate electron density reconstruction. For this purpose, the PEC estimates were modelled by a Chapman layer and an exponential decay function, as already mentioned. The PEC differences were corrected using the model's values and link geometries. The above-mentioned approach works when the RO data are not truncated; that means the sTEC data is available for the highest occultation ray perigee. However, this is not the case for the truncated data (see Figure 2).

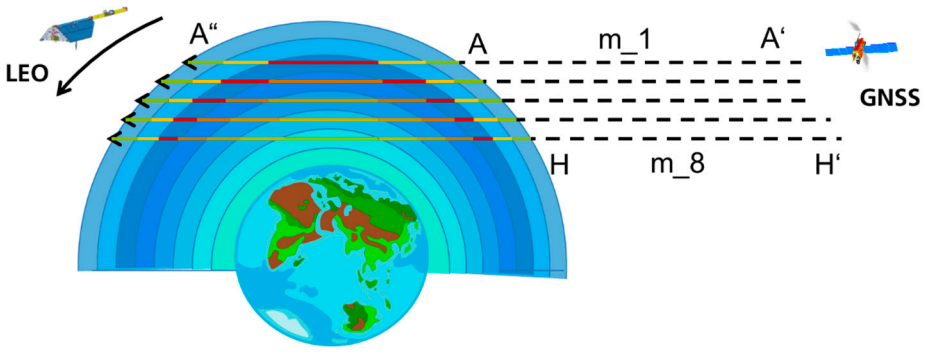

Figure 2. RO geometry with data truncation.

As shown in Figure 2, when the m_1 measurement is subtracted from the rest of the measurements, it not only removes the topside TEC (which is called the PEC here), the ambiguity and bias terms but also removes a constant TEC value corresponding to the A"A segment. For an accurate electron density reconstruction, a correction for the topside PEC differences, as well as a TEC correction for the A"A segment, need to be accomplished.

3. Initialization of topside model parameters:

As already mentioned, the topside model consists of a Chapman layer and an exponential decay function. The initial peak density height, *hm*, of the Chapman layer is obtained from an initial Abel inversion of the differential sTEC data. The peak density of the Chapman layer is initialized by Nm = TEC/(4.13Hs) [12], where the TEC is the vertical total electron content from the ground up to the GNSS's orbit height and is obtained from the empirical Neustrelitz TEC Model (NTCM, Refs. [13,14]). For the Chapman layer scale height, *Hs*, we used an initial value of 70 km, which is a moderate value for the scale height. The plasmaspheric basic density, *np*, is initialized by Nm/k, where k = 100 was assumed for the current reconstruction [4]. We compared the RO inversion results for other k values (e.g., k = 80, 120, 150, etc.), but their differences were not significant. Therefore, for simplicity, we fixed k = 100 for all of the cases. Future investigation can be conducted to find an optimum value of k using multi-instrument and multi-satellite measurements of the electron density in the ionosphere and plasmasphere. The plasmaspheric scale height, *Hsp*, is much higher than the Chapman layer scale height and can reach up to 10,000 km [4,15]. The *Hsp* is computed by using an empirical plasmasphere model called the Neustrelitz Plasmasphere Model (NPSM) [15].

4. The topside ionosphere–plasmasphere TEC contributions (e.g., the AA', . . . , HH' ray segments in Figure 2) were computed using the topside model (i.e., the Chapman layer plus the exponential decay function) initialized in the previous step. The TEC differences between the AA' segment and other segments were corrected. An Abel inversion was performed using such partially corrected measurements. An initial electron density profile was obtained, as shown in Figure 3.

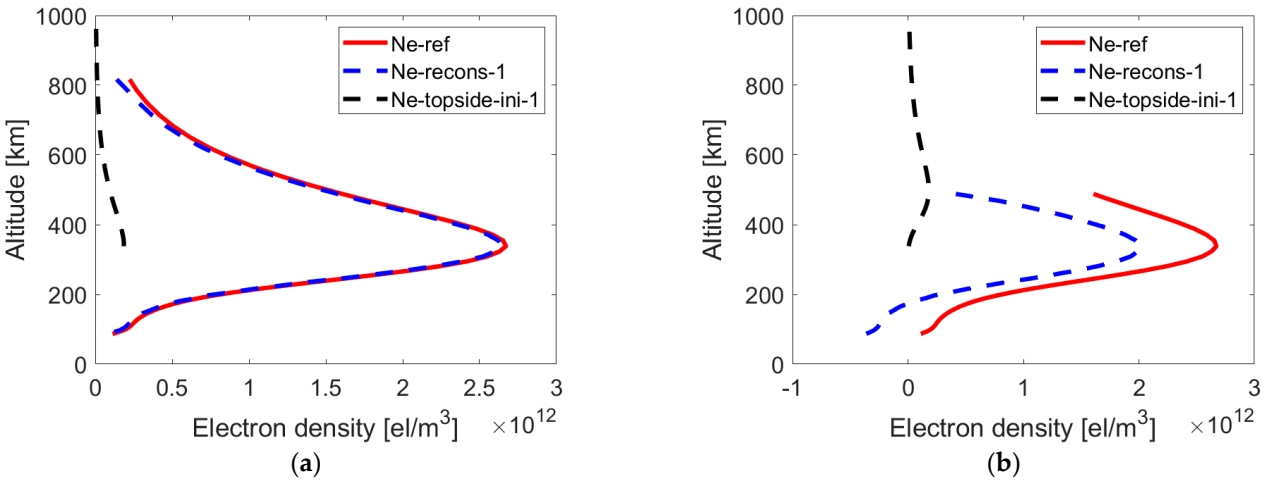

Figure 3. RO's inverted profiles (see blue, broken line curves) for a full dataset (Panel (**a**)) and a truncated dataset (Panel (**b**)). The red curve shows the reference Ne profile, and the black broken line curve shows the initial topside model.

Figure 3 shows the simulation results for an RO event where the geometry is arbitrarily taken from the COSMIC-1 mission data [7]. For the simulation, a reference electron density profile was modelled by combining three Chapman layers representing the ionospheric E, F1, and F2 layers and an exponential decay function for the plasmasphere [12] (see the red curve in Figure 3). First, the sTEC profile from this reference profile was computed for the

known geometry, and then the RO inversion technique was applied, as mentioned in steps 1–4. The left panel shows the initial inverted profile (see the blue curve) when the full sTEC dataset up to the LEO altitude (in the case of COSMIC-1, at about 800 km) was applied. In addition, the right panel shows the initial inverted profile (see the blue curve) when the same sTEC dataset was truncated at a 500 km altitude and used as the input. The black broken line curves show the initial topside model.

We note that although the initial topside model is not the correct one, the inverted profile is already very close to the reference profile when using a full dataset (see Figure 3a). However, in the case of the truncated dataset, the first inverted profile significantly differs from the reference profile.

5. Update of topside model parameters:

The topside model parameters *Nm*, *hm*, and *Hs* were determined from the inverted profile. It is noted that only the topside *Ne* data above the *hm* height were used for the scale height, *Hs*, determination. In case there is not enough topside *Ne* data available, the bottom part of the *Ne* data was used. In such a case, the data above the 150 km altitude were used to avoid any influence of the enhanced E-layer density. As before, the plasmaspheric scale height, *Hsp*, was obtained from the NPSM model.

Step 4 was repeated, and an Abel inversion was performed using the partially corrected measurements (by applying the updated topside model). An updated electron density profile was obtained, as shown in Figure 4.

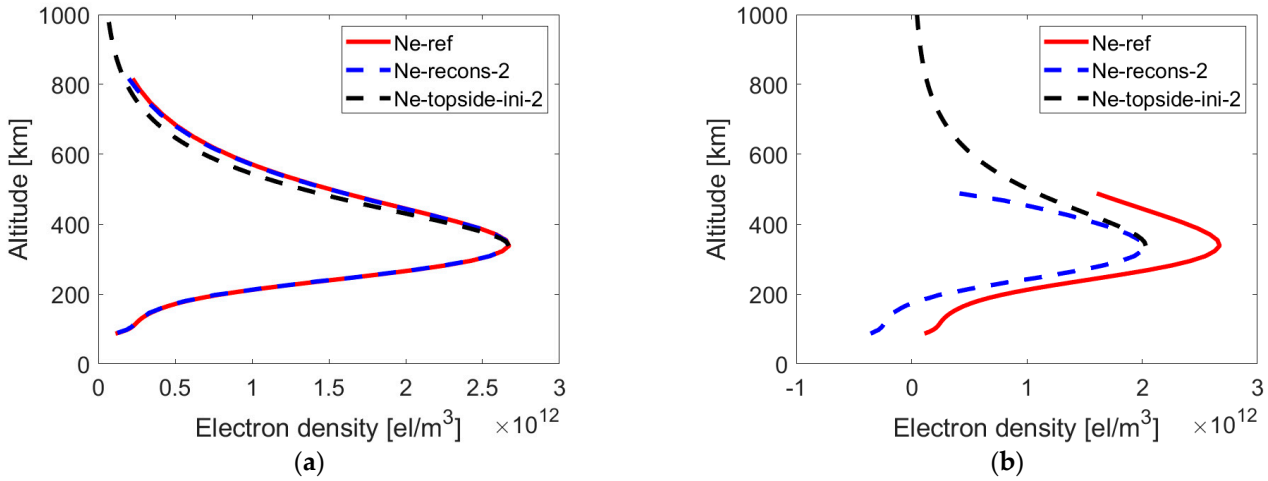

Figure 4. Updated RO inverted profiles (see blue, broken line curves) for a full dataset (Panel (**a**)) and a truncated dataset (Panel (**b**)).

As before, the red curve shows the same reference Ne profile, the black broken line curve shows the updated topside model, and the blue broken line curve shows the updated inverted profile.

The use of the updated topside model improves the RO inversion for the full dataset case, especially at higher altitudes over 600 km (see Figure 4a). However, the improvement for the truncated dataset case is not really visible (Figure 4b). The reason is that we have not yet corrected the TEC that corresponds to the A"A segment (see Figure 2).

6. Correction for data truncation

The correction for the data truncation (see the TEC contribution for the A"A segment in Figure 2) was computed using the topside model and applied together with Step 4. Another Abel inversion was performed using the corrected measurements, and an updated electron density profile was obtained, as shown in Figure 5.

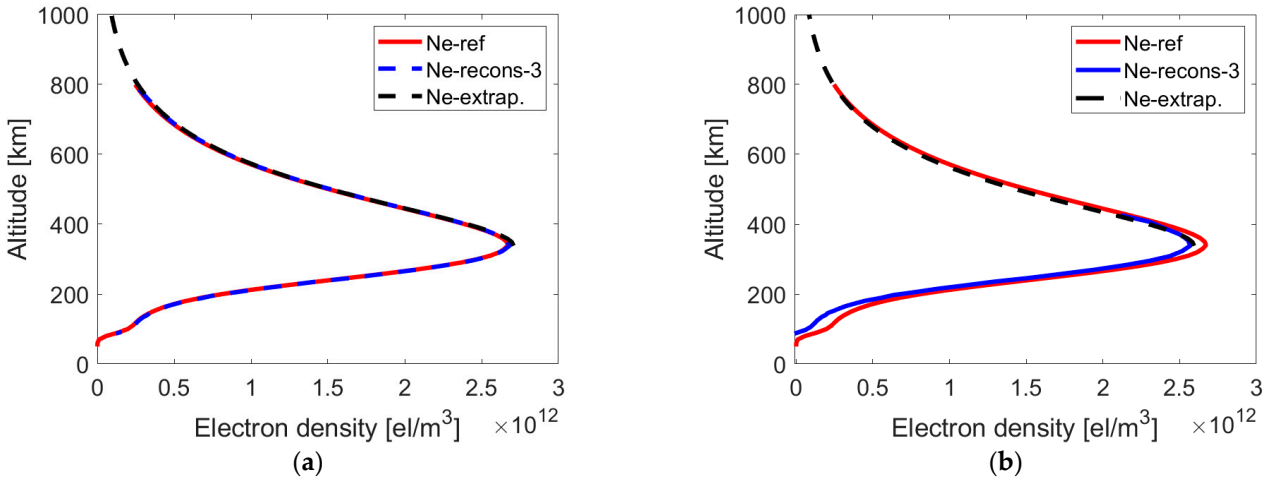

Figure 5. Updated RO inverted profiles (see blue line curves) for a full dataset (Panel (**a**)) and a truncated dataset (Panel (**b**)).

Figure 5 shows that the RO inversion for the truncated dataset improved significantly after applying the TEC correction for the A"A segment.

The topside model parameters were determined by three retrieval iterations to obtain a smooth transition between the model and the measurements at the upper boundary. Our investigation showed that further iterations did not show improvement in the reconstruction.

We have implemented the above-mentioned RO inversion method for the electron density reconstruction from the truncated RO data and analysed to what extent the limitation in the vertical measurement range has an impact on the data quality of the retrieved parameters in the following section.

3. Validation of RO Inversion Technique

The performance of the adaptive model's technique has been validated in terms of accuracy and computational load and power. The COSMIC-1 mission data [7,8] generated by the University Corporation for Atmospheric Research (UCAR) were used as independent references in the validation study. The validation was conducted in multiple ways, such as:

- The RO inversion technique was applied to the COSMIC-1 mission data. The data were intentionally truncated at a 600 km height. The RO inversion results were compared with the reference datasets. As the reference datasets, we used the RO profiles retrieved from the original datasets (i.e., the not truncated one) by the UCAR, as well as by the developed method;
- The RO inversion technique was applied to the COSMIC-1 mission data, further truncated at a 300 km height, and the RO inversion results were compared with the reference datasets;
- The RO inversion technique was then applied to the GRAS ionospheric extension experiment data, truncated at a 600 km height. The technique was also applied to the same GRAS data, further truncated at a 300 km height. The RO retrievals from the truncated data at 300 km were compared with the RO retrievals from the truncated data at a 600 km height.

3.1. Validation against COSMIC-1 Mission Data Truncated at 600 km

The advantage of using COSMIC-1 mission data is that the LEO orbit height is about 800 km (the data are collected up to that height), and we have options of applying the RO inversion technique for not only the artificially truncated data at 600 and 300 km height but also for the original data up to the LEO orbit height. The results obtained from the complete datasets can be used as truths for the RO inversions obtained from the truncated data.

For validation purposes, we arbitrarily used COSMIC-1's sTEC profiles for the Day Of Year (DOY) 348, 2011. The developed RO inversion technique was applied to the full datasets as well as to the truncated datasets.

Figure 6 shows a comparison between the RO retrieval using the full datasets up to the LEO orbit height (see the red and green curves levelled as "orig-ucar" and "orig-dlr") and the RO retrieval using the truncated datasets (see the blue and magenta curves levelled as "truncat-600 km" and "truncat-300 km").

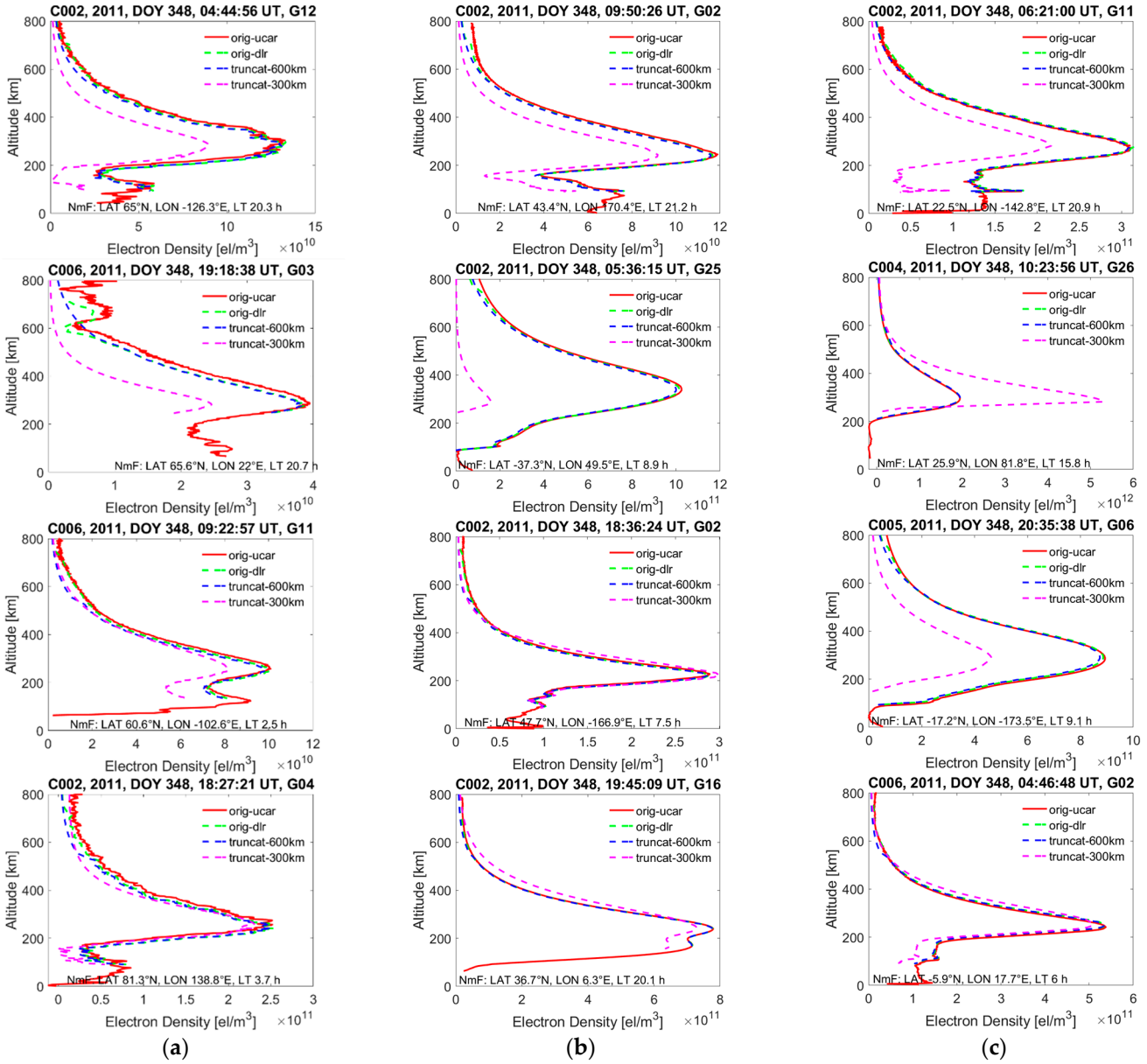

Figure 6. RO retrieval using COSMIC-1 mission data. Red and green colored curves denote RO inversion using full datasets (i.e., up to the LEO orbit height) by the UCAR and proposed method, respectively. The blue broken line curve shows RO inversion from truncated data at 600 km, and the magenta broken line curve shows RO inversion from the truncated data at 300 km. Panels (**a**–**c**) show example plots from high, middle, and low latitude regions.

Our investigation, based on over 600 RO inverted profiles from the COSMIC-1 RO data for that day, shows that the developed technique performs well. When comparing the results of the inversion of the data truncated at 600 km (the dashed blue curves) with

the reference Ne profiles obtained from the full datasets (see the red and green curves), we see that below the 600 km altitude, the Ne retrieval performs very well. Above the 600 km altitude level, the retrieval underestimates the Ne values in some cases. It might be that the assumed plasmaspheric scale height was smaller than the actual one, so the topside electron density fell sharply at the upper height. Other reasons might be that the factor $k = 100$, used in the assumption of np (i.e., Nm/k), was too large so that the basic density, np, became smaller than it should have been, which in turn caused an underestimation of the electron density throughout the topside ionosphere and plasmasphere. It is expected that the Ne reconstruction will be improved by proper approximations of the plasmaspheric basic density and scale height. Future research can be directed to find a way of approximating an optimum value of k depending on geophysical conditions. It was found that for many of the cases, the developed inversion method slightly underestimates the peak density value. A more careful look shows that the inversion performs very well up to the peak density height. That means, in most cases, the RO retrieval in the bottom part is almost not affected by the data truncation.

Above the peak density height, the retrieval accuracy started decreasing. Such degradation in accuracy is expected since the data were truncated at the upper height. The usage of full datasets has mainly two advantages: (1) the additional topside data help to estimate the topside model parameters more accurately, and (2) the influence of the unknown topside ionospheric and plasmaspheric part in the overall RO inversion is less.

The second plot (from the top) in Panel (a) clearly shows that the inversion fails to reconstruct the sudden change in the electron density distribution above the 600 km altitude level. Since we were predicting and extrapolating the topside above the truncated height of 600 km, the prediction could not reproduce the actual fluctuations in the data.

In order to analyse the performance of the inversion technique, the Ne profile data were preprocessed to compute the electron density values from 90 km up to 550 km, with a step size of 20 km. This was conducted by applying the spline interpolation to the original Ne profile data obtained by the UCAR and DLR and the Ne profiles retrieved from the RO data truncated at 600 km and 300 km heights. The percentage differences in the reconstructed Ne with respect to the reference Ne data were determined at each specified height level (i.e., between 90–550 km, with a step size of 20 km) by the following formula:

$$perc\_diff = \frac{(Ne_{recon} - Ne_{ref})*100\%}{Ne_{ref}} \quad (6)$$

where Ne_{recon} is the reconstructed electron density at a specific height from the truncated data, and Ne_{ref} is the reference electron density, or the truth value, at the same height, which was obtained by either the UCAR or the DLR method by applying the complete RO datasets (i.e., no data truncation). Thus, such percentage difference profiles were computed for all of the reconstructed profiles obtained from the truncated data. Then, the root mean square (RMS) and standard deviation (STD) values of the percentage differences were computed at each height level for the height region between 90 and 550 km, considering all available profiles, and plotted in Figure 7.

Figure 7a shows that the RMS and STD differences along the altitude are smaller when compared with the DLR references (see the red and blue continuous line plots). We have found that the RMS difference varies between 4 and 11%, and the mean RMS difference is about 7%, whereas the STD difference varies between 3 and 7%, and the mean STD difference is about 4.3%. When compared with the UCAR reference data, we have found that the RMS difference varies between 7 and 16%, and the mean RMS value is about 11%. The STD difference varies between 8.5 and 14.5%, and the mean STD difference is found at about 8.6%. As expected, we found that the RMS and STD differences were larger when the inversion results (from the truncated data) were compared with the UCAR data. The reason is that the Abel inversion technique, as reported in [8,16,17] and used by the UCAR, is not the same as the DLR one. The UCAR approach does not use any topside ionosphere and plasmasphere models for electron density retrieval from the COSMIC

data. Schreiner et al. [17] found that the RO inversion results were slightly different when calibrated slant TEC data were used instead of uncalibrated data as the inputs to the Abel inversion. Recently, Pedatella et al. [18] used a monthly grid of the F region peak densities (Nm) to aid the Abel inversion by providing information on the horizontal gradients in the ionosphere. They found that the Nm-aided retrieval significantly improved the quality of the COSMIC electron density profiles.

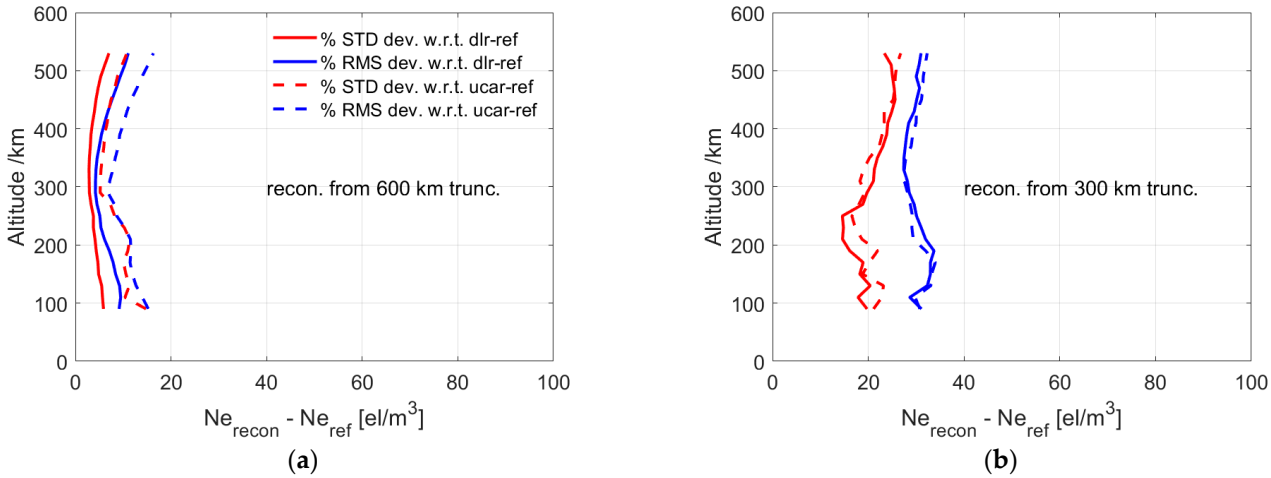

Figure 7. Performance analysis of reconstructed profiles (**a**) from the 600 km truncated data and (**b**) from the 300 km truncated data, in terms of RMS and STD of the percentage differences, with respect to the reference Ne profiles.

3.2. Validation against COSMIC-1 Mission Data Truncated at 300 km

We also tested the performance of the RO inversion technique when it was applied to the truncated data at the 300 km height.

The above investigation was repeated for the Ne profiles obtained from the truncated data at the 300 km height (see Figure 7b). We have found that the RMS differences are quite similar, varying between 27–33% with respect to both reference datasets. The mean RMS difference is found at about 30%. The STD differences vary between 15–26%, and the mean STD difference is found at about 21% for both reference datasets. As expected, we found larger RMS and STD differences for the 300 km-truncated case compared to the 600 km case.

A literature study shows that the peak ionization height of the F2 layer may lie between 250 and 450 km of height above the Earth's surface. So, if we truncate the data at the 300 km height, in many cases, we only have information about the bottom part of the electron density distribution. It may happen that the peak density will be missed in the remaining data after the truncation. As discussed in the previous sections, a successful RO inversion requires corrections for the topside ionospheric and plasmaspheric contribution. Therefore, if the topside data (an altitude > *hm* height) is completely missing, the topside contribution cannot be correctly estimated. Therefore, the RO inversion using the truncated data at the 300 km height is very challenging. Nevertheless, we applied the technique to the truncated data, and we found very mixed results. In many cases, the RO inversion cannot retrieve the electron density profiles accurately. However, in some cases, the performance of the model-assisted technique is good, and the retrieved profile is close to the reference profile.

Figure 6 (see the magenta curves) shows some examples of the retrieved electron density profiles using the truncated data at the 300 km height. Again, the RO retrievals derived using the full, not truncated datasets (the red and green curves) can be treated as the reference. Additionally, the retrieved profiles from the truncation at 600 km (the blue curves) can be used for comparison. We see that in many cases, the retrieval (for the truncation at 300 km) underestimates, and in some cases, it overestimates the reference values. The

investigation shows that the underestimation of the topside electron density occurs more frequently than the overestimation, as expected. As described in Section 2, when the topside data are missing in the truncated data, the topside scale height is computed from the bottom side data. However, the scale height inferred from the bottom side is lower than from the topside. Considering this, we could expect that the profiles modelled from the truncated profiles at 300 km should always underestimate the topside. However, we found that although in most cases, the retrieval was underestimated, in a number of cases, it overestimated the reference Ne values. One reason may be that the peak electron density, *Nm*, is highly overestimated when it is initialized by the Chapman layer assumption, together with the NTCM model and an average scale height value of 70 km. Consequently, the plasmaspheric basic density, *np*, might have been overestimated, which caused the overall overestimation of the topside ionosphere. It is difficult to say when the retrieved profile is accurate or when it is not accurate, and more investigation is needed to characterize the accuracy of the retrieved profiles. Anyway, our investigation shows that the model-assisted technique works (in the sense that it provides output) for retrieving an electron density profile from the truncated data at 300 km. As already discussed, in many cases, the sTEC data from the topside part is very limited or even completely missing. In such a case, the topside Chapman layer scale height is computed from the bottom part of the profile. In any case, for the scale height computation, we did not use the data below the 150 km height level to avoid any influence of the enhanced E-layer density.

Therefore, we conclude that the truncation at the 300 km height has a high impact on the accuracy of the inverted profiles. The accuracy significantly degrades in most cases. We found that the main advantage of the model-assisted technique is that it works and is able to produce electron density profiles, in most cases, if the peak height is lower than 300 km.

3.3. First Results of RO Inversion Using MetOp-A's Experiment Data Truncated at 600 km and 300 km

We applied the developed method to the GRAS data collected during the ionospheric extension experiment, and we obtained very promising results. In this paper, we used the data originally acquired up to the 600 km height. However, to test the retrieval technique, we also intentionally further truncated the same dataset at the 300 km height. Both data sets, i.e., the data truncated at the 600 km and 300 km heights, were fed into the inversion process. Thus, the retrieval results obtained from the truncated data at the 600 km height were used as the reference data sets for validating the retrieval results from the truncated data at the 300 km height.

We arbitrarily chose data from the DOY 211, 2020 and computed 1 Hz of the sTEC profile using the dual-frequency carrier phase measurements. The 1 Hz data were computed from 50 Hz of data, taking the first measurement value during each 1 s period. The 1 Hz of sTEC data was then fed into the RO inversion process. The retrieval results are presented in Figure 8, based on the observation location over high (60–90°), middle (30–60°), and low (0–30°) latitude regions in Panels (a), (b), and (c), respectively.

Figure 8 shows that in some cases, the retrieval results from the truncated data at the 300 km height are comparable to the retrieval results from the truncated data at 600 km. Our investigation also shows that the retrieval can successfully retrieve E-layer Dominated Ionosphere (ELDI) electron density profiles. In such a case, the peak electron density occurs at the E-layer's height (90–150 km) instead of the F-layer's height (see the plots in Panel a). The occurrence probability of the ELDI profiles, and their geographic distribution, are explicitly discussed in [19–21].

In some cases, the retrieved profiles from the truncated data at 300 km largely differ from the profiles retrieved from the truncated data at 600 km of height. In such cases, underestimation is observed more frequently than overestimation of the electron density.

We found that in many cases, the E-layer's density was correctly retrieved, although the F-layer's density suffered significant deviations from the reference values (i.e., the

retrievals from the datasets truncated at 600 km of height). In general, as expected, the retrieval works fine when the peak density height lies far below the 300 km height.

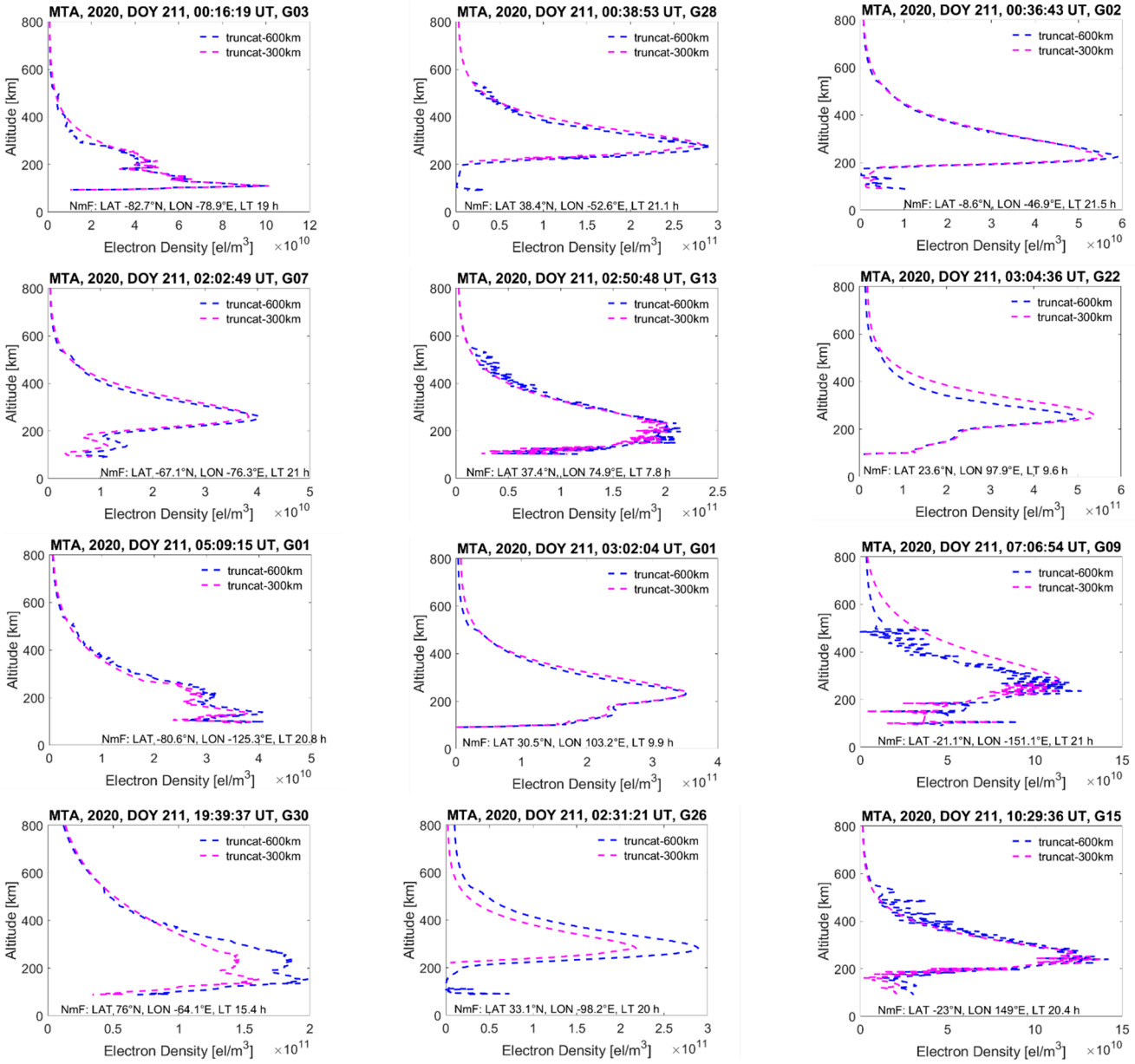

Figure 8. Blue and magenta broken line curves show the retrieval using truncated data at 600 and 300 km from MetOp-A's extension experiment. Panels (**a**–**c**) show retrieval examples over high (60–90°), middle (30–60°), and low (0–30°) latitude regions, respectively.

The peak density height gradually increases when moving towards the middle and low latitude regions from the high latitude region. Due to this, the peak density height mostly lies over the 250 km altitude. However, the peak density occasionally lies at around 200 km of height. In such cases, the retrieval from the truncated data at 300 km performs well. At the middle and low latitude regions (the plots in panels b and c), we found that in many cases, the retrieval could correctly reconstruct the E-layer's density, although the F-layer's density deviated largely from the reference values. In such cases, the density representing the topside ionosphere–plasmasphere suffers the most. When the data are truncated around or below the peak density height, the topside ionosphere–plasmasphere

part cannot be successfully modelled. Due to this, the accuracy of the retrieval technique degrades as expected.

Our investigation shows that the model-assisted technique is stable and robust. Even with the help of a small amount of data on the topside above the peak density height, the technique can predict the profile up to the LEO height. If the peak density lies below the 250 km altitude level, the accuracy of the retrieved profile is comparable to the accuracy of the retrieved profile from the truncated data at the 600 km height. The peak density of the retrieved profile can be known from the profile data. Therefore, such profiles can be useful. The ELDI profile generated from the truncated data can be readily used for an ELDI investigation due to the presence of the peak density at a lower height below the 140 km level.

We found that the computational cost and demand for the adaptive model approach are very low. The runtime for reconstructing a single profile is found in about a few seconds. A realistic topside model assumption makes the adaptive model approach stable. Our investigation shows that the implementation of the adaptive model technique is suitable for operational use with respect to memory use, computational power, and timeliness.

4. Conclusions

We developed a model-assisted inversion technique for electron density retrieval from MetOp-A's RO measurements. MetOp-A's RO measurements were only taken with an impact parameter height below 600 and 300 km, although MetOp-A was flying at an orbit height of about 800 km. However, a successful electron density retrieval requires a topside ionosphere and plasmasphere contribution above 600/300 km of altitude to be correctly modelled. Considering this, the topside ionosphere and plasmasphere above the LEO orbit height were modelled by a Chapman layer function superposed with an exponential decay function representing the plasmasphere. The performance of the adaptive model technique was tested using simulated data as well as COSMIC-1's RO data. After successful validation against the COSMIC-1 data, the RO inversion method was applied to the MetOp-A's truncated data at 600 km and 300 km. We found that if the peak electron density lies below the 250 km altitude level, the accuracy of the retrieved profile from the data truncation at 300 km is comparable to the accuracy of the retrieved profile from the truncated data at 600 km of height. Our investigation shows that the model-assisted technique is stable and robust. Even with the availability of a small amount of data on the topside above the peak density height, the technique can predict the profile up to the LEO orbit height. Our investigation shows that the computational cost and demand for the developed model approach are very low. The runtime for reconstructing a single profile is found in about a few seconds. The developed RO inversion technique is suitable for operational use with respect to memory use, computational power, and timeliness.

Author Contributions: Conceptualization, M.M.H.; Data curation, A.V.E. and C.M.; Funding acquisition, M.M.H.; Investigation, F.S.P., M.H.-P. and N.J.; Methodology, M.M.H. and L.Y.; Project administration, R.N., A.V.E. and C.M.; Software, M.M.H.; Validation, M.M.H. and L.Y.; Writing—original draft, M.M.H.; Writing—review & editing, M.M.H., F.S.P., M.H.-P., R.N., N.J., G.O.P. and A.V.E. All authors have read and agreed to the published version of the manuscript.

Funding: This research was funded by the EUMETSAT, contract EUM/CO/21/4600002530/RN, within the project named the Assessment of GRAS Ionospheric Measurements for Ionospheric Model Assimilation (GIMA).

Data Availability Statement: The used COSMIC 1 data are available at the UCAR site https://www.cosmic.ucar.edu/what-we-do/cosmic-1/data (accessed on 28 January 2023). All data used within this study (the GRAS/MetOp-A products, including the dual-frequency bending angles, scintillation index profiles, and topside TEC) are considered 'essential' data under the EUMETSAT data policy. Consequently, they can be made available on a free and unrestricted basis. In case you are interested, please contact the EUMETSAT user helpdesk (ops@eumetsat.int).

Acknowledgments: The authors would like to thank the University Corporation for Atmospheric Research, Boulder, CO, USA, and the National Space Organization, Hsinchu, Taiwan, for providing the COSMIC/FORMOSAT data.

Conflicts of Interest: The authors declare no conflict of interest.

References

1. Hernandez-Pajares, M.; Juan, J.M.; Sanz, J. Improving the Abel inversion by adding ground data LEO radio occultations in the ionospheric sounding. *Geophys. Res. Lett.* **2000**, *27*, 2743–2746. [CrossRef]
2. Garcia-Fernandez, M.; Hernandez-Pajares, M.; Juan, J.M.; Sanz, J. Improvement of ionospheric electron density estimation with GPSMET occultations using Abel inversion and VTEC information. *J. Geophys. Res.* **2003**, *108*, 1338. [CrossRef]
3. Jakowski, N.; Wehrenpfennig, A.; Heise, S.; Reigber, C.; Lühr, H.; Grunwaldt, L.; Meehan, T. GPS radio occultation measurements of the ionosphere from CHAMP: Early results. *Geophys. Res. Lett.* **2002**, *29*, 1457. [CrossRef]
4. Jakowski, N. Ionospheric GPS radio occultation measurements on board CHAMP. *GPS Solut.* **2005**, *9*, 88–95. [CrossRef]
5. Hernández-Pajares, M.; Garcia-Fernàndez, M.; Rius, A.; Notarpietro, R.; von Engeln, A.; Olivares-Pulido, G.; Aragón-Àngel, À.; García-Rigo, A. Electron density extrapolation above F2 peak by the linear Vary-Chap model supporting new Global Navigation Satellite Systems-LEO occultation missions. *J. Geophys. Res. Space Phys.* **2017**, *122*, 9003–9014. [CrossRef]
6. Lyu, H.; Hernández-Pajares, M.; Monte-Moreno, E.; Cardellach, E. Electron density retrieval from truncated radio occultation GNSS data. *J. Geophys. Res. Space Phys.* **2019**, *124*, 4842–4851. [CrossRef]
7. UCAR/NCAR—COSMIC. UCAR COSMIC Program, 2006: COSMIC-1 Data Products 'podTec' and 'ionPrf'. Available online: https://www.cosmic.ucar.edu/what-we-do/cosmic-1/data (accessed on 28 January 2023).
8. Syndergaard, S.; Schreiner, W.S.; Rocken, C.; Hunt, D.C.; Dymond, K.F. Preparing for COSMIC: Inversion and analysis of ionospheric data products. In *Atmosphere and Climate*; Foelsche, U., Kirchengast, G., Steiner, A., Eds.; Springer: Berlin/Heidelberg, Germany, 2006. [CrossRef]
9. Rishbeth, H.; Garriott, O.K. *Introduction to Ionospheric Physics*; Academic Press: New York, NY, USA, 1969.
10. Prol, F.S.; Themens, D.R.; Hernández-Pajares, M.; de Oliveira Camargo, P.; Muella, M.T.D.A.H. Linear Vary-Chap topside electron density model with topside sounder and radio-occultation data. *Surv. Geophys.* **2019**, *40*, 277–293. [CrossRef]
11. Prol1, F.S.; Smirnov, A.G.; Hoque, M.M.; Shprits, Y.Y. Combined model of topside ionosphere and plasmasphere derived from radio-occultation and Van Allen Probes data. *Nat. Sci. Rep.* **2022**, *12*, 9732. [CrossRef] [PubMed]
12. Hoque, M.M.; Jakowski, N. Mitigation of higher order ionospheric effects on GNSS users in Europe. *GPS Solut.* **2007**, *12*, 87–97. [CrossRef]
13. Jakowski, N.; Hoque, M.M.; Mayer, C. A new global TEC model for estimating transionospheric radio wave propagation errors. *J. Geod.* **2011**, *85*, 965–974. [CrossRef]
14. Hoque, M.M.; Jakowski, N. An Alternative Ionospheric Correction Model for Global Navigation Satellite Systems. *J. Geod.* **2015**, *89*, 391–406. [CrossRef]
15. Jakowski, N.; Hoque, M.M. A new electron density model of the plasmasphere for operational applications and services. *J. Space Weather Space Clim.* **2018**, *8*, A16. [CrossRef]
16. Schreiner, W.S.; Sokolovskiy, S.V.; Rocken, C.; Hunt, D.C. Analysis and validation of GPS/MET radio occultation data in the iono-sphere. *Radio Sci.* **1999**, *34*, 949–966. [CrossRef]
17. Schreiner, W.S.; Rocken, C.; Sokolovskiy, S.; Syndergaard, S.; Hunt, D. Estimates of the precision of GPS radio occultations from the COSMIC/FORMOSAT-3 mission. *Geophys. Res. Lett.* **2007**, *34*, L04808. [CrossRef]
18. Pedatella, N.M.; Yue, X.; Schreiner, W.S. An improved inversion for FORMOSAT-3/COSMIC ionosphere electron density profiles. *J. Geophys. Res. Space Phys.* **2015**, *120*, 8942–8953. [CrossRef]
19. Mayer, C.; Jakowski, N. Enhanced E-layer ionization in the auroral zones observed by radio occultation measurements onboard CHAMP and Formosat-3/COSMIC. *Ann. Geophys.* **2009**, *27*, 1207–1212. [CrossRef]
20. Kamal, S.; Jakowski, N.; Hoque, M.M.; Wickert, J. Evaluation of E Layer Dominated Ionosphere Events Using COSMIC/FORMOSAT-3 and CHAMP Ionospheric Radio Occultation Data. *Remote Sens.* **2020**, *12*, 333. [CrossRef]
21. Kamal, S.; Jakowski, N.; Hoque, M.M.; Wickert, J. E Layer Dominated Ionosphere Occurrences as a Function of Geophysical and Space Weather Conditions. *Remote Sens.* **2020**, *12*, 4109. [CrossRef]